

<sup>1</sup> **Supplementary Information for “More positive and  
2 less variable North Atlantic Oscillation at high CO<sub>2</sub>  
3 forcing”**

<sup>4</sup> **Ivan Mitevski<sup>1,\*</sup>, Simon H. Lee<sup>2</sup>, Gabriel Vecchi<sup>1,3</sup>, Clara Orbe<sup>4,5</sup>, and Lorenzo M. Polvani<sup>5,6</sup>**

<sup>5</sup> <sup>1</sup>Geoscience Department, Princeton University, NJ, USA

<sup>6</sup> <sup>2</sup>School of Earth and Environmental Sciences, University of St Andrews, St Andrews, UK

<sup>7</sup> <sup>3</sup>High Meadows Environmental Institute, Princeton University, NJ, USA

<sup>8</sup> <sup>4</sup>NASA Goddard Institute for Space Studies, New York, NY, , USA

<sup>9</sup> <sup>5</sup>Department of Applied Physics and Applied Mathematics, Columbia University, New York, NY, , USA

<sup>10</sup> <sup>6</sup>Lamont-Doherty Earth Observatory, Columbia University, Palisades, NY

<sup>11</sup>\* e-mail: mitevski@princeton.edu

<sup>12</sup> **ABSTRACT**

<sup>13</sup>

Model	2×CO <sub>2</sub>	4×CO <sub>2</sub>	8×CO <sub>2</sub>
CESM-LE	×	×	×
GISS-E2.1-G	×	×	×
GFDL-FLOR	×	×	
CCSM3	×	×	×
CESM104	×	×	×
CNRMCM61	×	×	
ECEARTH		×	
ECHAM5MPIOM		×	
GFDLCM3	×		
GFDLESM2M	×		
GISSE2R		×	
HadCM3L	×	×	×
IPSLCM5A		×	
MIROC32	×	×	
MPIESM12	×	×	×
ACCESS-CM2		×	
ACCESS-ESM1-5		×	
AWI-CM-1-1-MR		×	
BCC-CSM2-MR		×	
CAMS-CSM1-0		×	
CESM2-WACCM		×	
E3SM-1-0		×	
EC-Earth3		×	
EC-Earth3-Veg		×	
FGOALS-f3-L		×	
FGOALS-g3		×	
GFDL-CM4		×	
GFDL-ESM4		×	
IITM-ESM		×	
INM-CM4-8		×	
INM-CM5-0		×	
KACE-1-0-G		×	
MPI-ESM1-2-HR		×	
MPI-ESM1-2-LR		×	
NorESM2-MM		×	
TaiESM1		×	
CESM2		×	
GISS-E2-1-H		×	
IPSL-CM6A-LR		×	
MIROC6	×	×	
MRI-ESM2-0	×	×	
BCC-ESM1		×	
CanESM5		×	
CESM2-FV2		×	
CIESM		×	
EC-Earth3-CC		×	
FIO-ESM-2-0		×	
GISS-E2-2-G		×	
GISS-E2-2-H		×	
IPSL-CM5A2-INCA		×	
KIOST-ESM		×	
MCM-UA-1-0		×	
MPI-ESM1-2-HAM		×	
NESM3		×	
NorCPM1		×	
NorESM2-LM		×	
SAM0-UNICON		×	
Total models			

**Table 1.** Models and experiments used in the NAO calculations in the main text. The “×” denotes experiments available for each model.

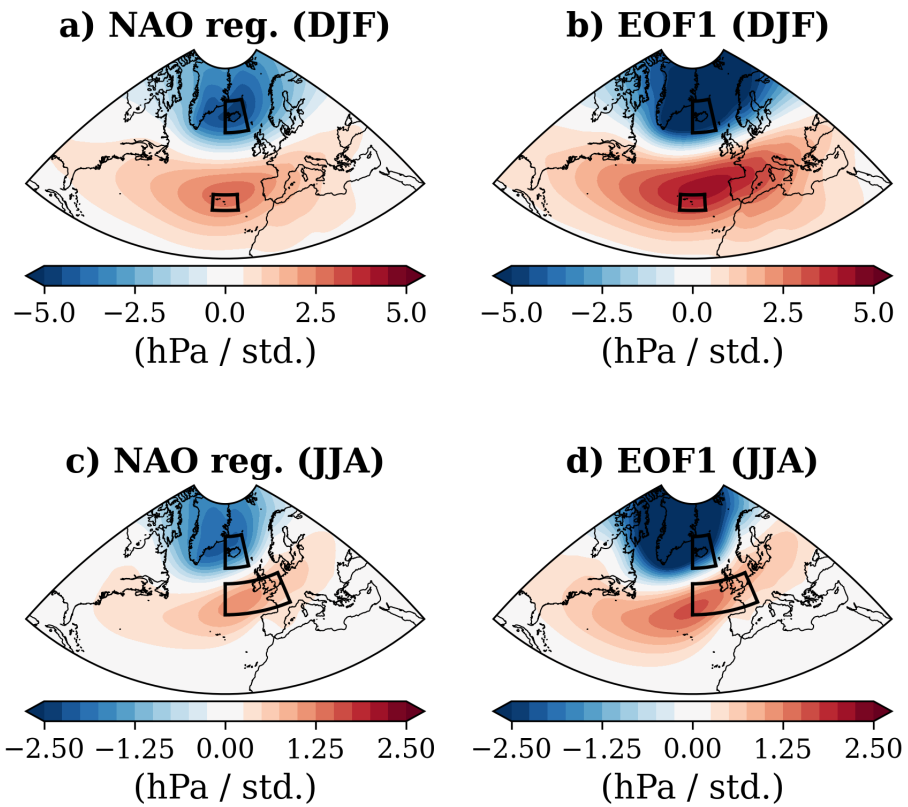


**Figure S1: North Atlantic Oscillation (NAO) regression patterns.** The mean sea level pressure (SLP) at each latitude and longitude is regressed onto the standardized NAO index, defined using the difference between the SLP in the two boxes (southern minus northern), for (a) DJF and (c) JJA. In (b) and (d), the NAO is instead computed as EOF1 of the SLP field in the domain. The figure shows the multi-model mean regression pattern obtained from preindustrial (PI) control runs.

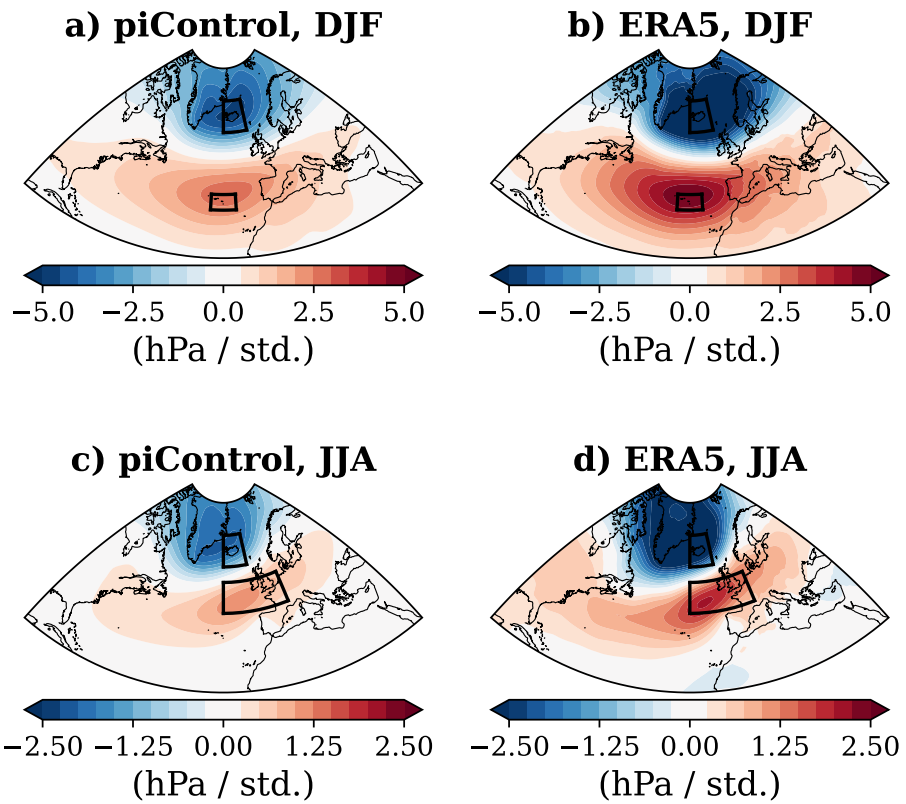


**Figure S2: Comparison between modeled and reanalysis NAO patterns.** The multi-model mean PI control regression patterns are shown in (a) for DJF and (c) for JJA. (b) and (d) show equivalent maps but using ERA5 reanalysis over (b) 1979/80–2023/24 and (d) 1979–2023.

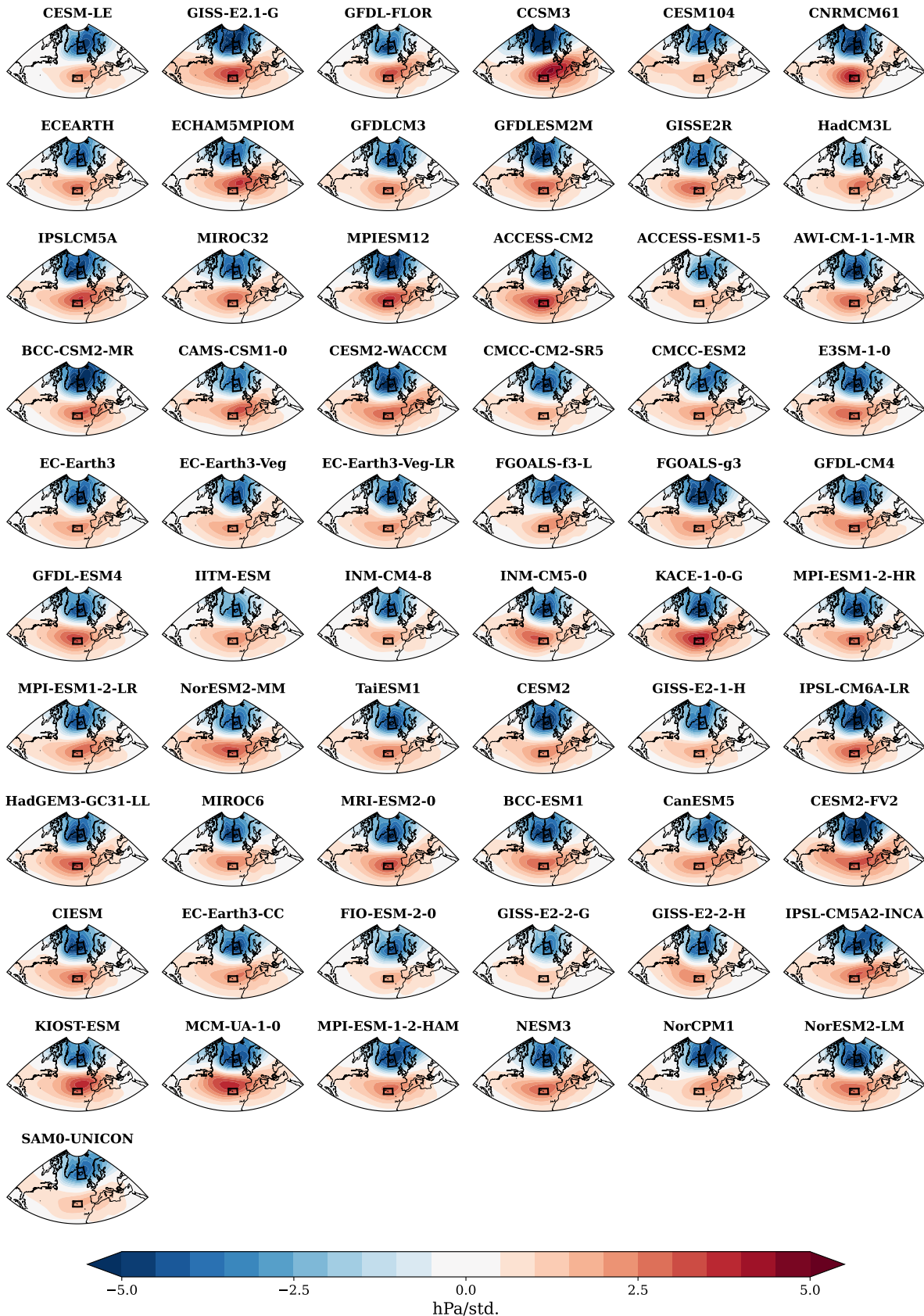


**Figure S3: Individual model DJF NAO regression patterns using the PI control experiments.**

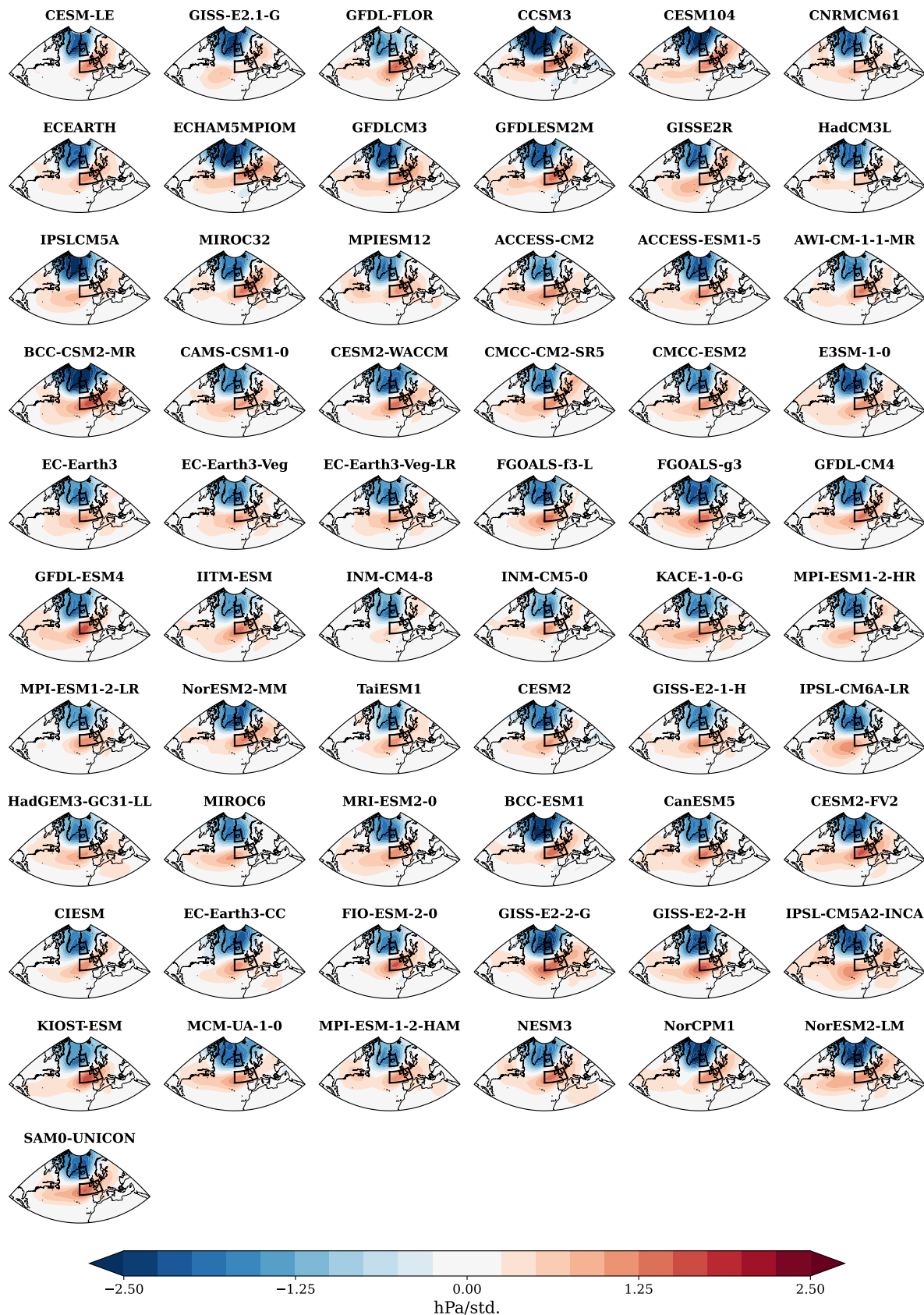


**Figure S4: Individual model JJA NAO regression patterns using the PI control experiments.**

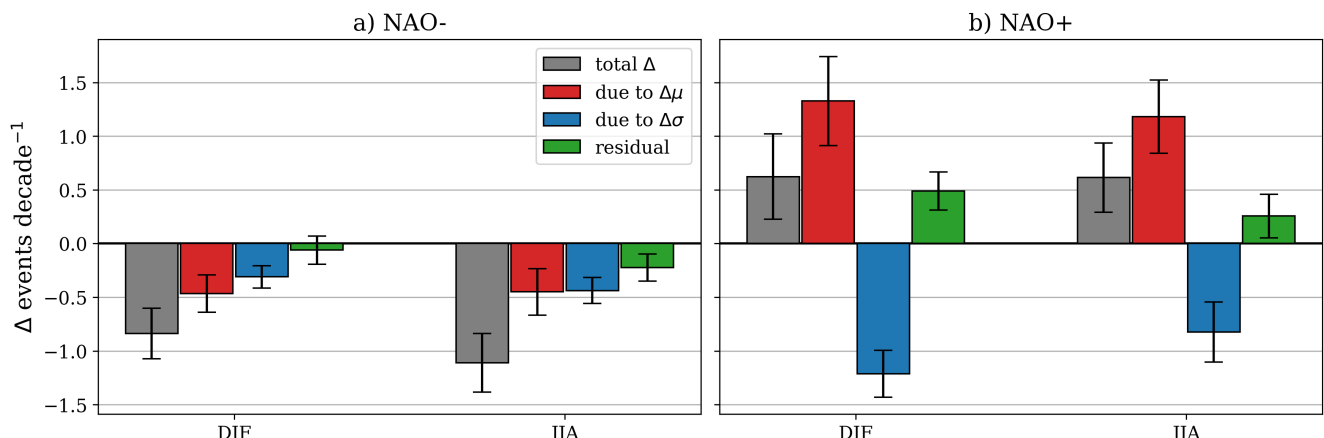


**Figure S5: Change in extreme NAO events at  $4\times\text{CO}_2$  using a threshold of  $1.5\sigma$ .** Extreme (a) NAO– and (b) NAO+ events for DJF (first set of bars) and JJA (second set of bars). The total change (gray) is decomposed into contributions due to shift in NAO mean (red), standard deviation (blue) and due to the non-normality of the distribution (green).